

A Calcium-Modulated Plasmonic Switch

W. Paige Hall,[†] Jeffrey N. Anker,[†] Yao Lin,^{‡,§} Justin Modica,[‡] Milan Mrksich,[‡] and Richard P. Van Duyne^{*,†}

Department of Chemistry, Northwestern University, 2145 Sheridan Road, Evanston, Illinois 60208, Department of Chemistry, University of Chicago, 929 East 57th Street, Chicago, Illinois 60637, and Biosciences Division, Argonne National Laboratory, 9700 South Cass Avenue, Argonne, Illinois 60439

Received December 6, 2007; E-mail: vanduyne@northwestern.edu

Cellular activities are mediated by proteins, which often undergo conformational changes to regulate binding and enzymatic activities that direct signaling pathways. Hence, it is important to develop and apply tools to characterize dynamic changes in protein conformation. A variety of approaches are available, including those based on NMR,¹ FRET,² and plasmonics.^{3,4} Plasmonic approaches are particularly useful because they provide an intense signal that does not bleach and allow nondestructive measurement over long periods of time. In addition to acting as probes of molecular interactions, plasmonic devices have significant potential as nanoscale optical switches, waveguides, light sources, microscopes, and lithographic tools.^{3,4} Herein, we demonstrate a plasmonic switching device based on the calcium-induced conformational changes of calmodulin. The extinction maximum (λ_{max}) of a localized surface plasmon resonance (LSPR) sensor functionalized with calmodulin reversibly shifts by 2–3 nm in response to changes in Ca^{2+} concentration, creating a unique on/off switch and providing information about the dynamics and structure of the protein. A high-resolution (HR) LSPR spectrometer with a wavelength resolution (3σ) of 1.5×10^{-2} nm was used to detect the calcium-modulated wavelength shifts (Supporting Information).

The LSPR is a unique nanoscale phenomenon that gives rise to an intense extinction and scattering spectrum in noble metal nanoparticles that is highly dependent on the local refractive index at the nanoparticle surface. Biomolecule adsorption to a nanoparticle alters the local refractive index, causing shifts in the extinction maximum (λ_{max}). The magnitude and direction of these shifts provide detailed information about the packing density of the adsorbed species.⁵ LSPR sensors can be used to characterize and detect a wide variety of biological events, including DNA hybridization,⁶ carbohydrate–protein binding,⁷ and antigen–antibody interactions.^{8,9}

A commercially established technology based on propagating SPR in thin Au films can sense changes in refractive index up to 1 μm away from the sensor surface. Such SPR sensors have been used to detect protein conformational changes due to denaturation.^{10,11} However, the relatively large sensing region of propagating SPR sensors gives rise to interference from bulk refractive index changes. In contrast, the LSPR sensing region in Ag nanoparticles is confined to a thin (25–30 nm) shell around the nanoparticle.¹² As a result, LSPR sensors possess 40-fold greater spatial resolution normal to the sensor surface, allowing improved detection of low molecular weight binding events. Monitoring LSPR changes in real-time provides information about the dynamics of binding events and protein folding, with much less interference from bulk refractive index changes.

Despite the superior spatial resolution of LSPR sensors, low S/N ratios have presented a challenge. However, developments in instrumentation and data analysis have dramatically improved the sensitivity of LSPR sensors, enabling real-time detection in solution. For example, Höök et al. developed a sensor capable of measuring LSPR shifts of less than 5×10^{-4} nm to detect binding to nanohole films.¹³ This level of sensitivity is comparable to propagating SPR sensors in terms of shift/molecule/area. Using single nanoparticles, LSPR spectroscopy has the potential to surpass the sensitivity of SPR.¹⁴

In this work, we use an HR LSPR spectrometer to detect binding and conformational changes in real-time with a standard deviation in LSPR wavelength of 5×10^{-3} nm for nanosphere lithography (NSL)-fabricated Ag nanoprisms arrays incubated in solution. While this noise level is 10-fold higher than that reported by Höök, in part because nanoholes absorb more light than NSL arrays, the shift per molecule is higher for NSL arrays due to their shorter electromagnetic field decay length,⁶ resulting in a similar overall sensitivity per molecule. This noise level corresponds to a S/N ratio of 800 for typical (MW \sim 60 kDa) protein binding events, facilitating measurement of binding rates.

To demonstrate the capabilities of our real-time, HR LSPR spectrometer, we characterized the calcium-dependent conformational change in calmodulin (CaM), a protein that mediates many cellular responses to the second messenger calcium ion. CaM binds Ca^{2+} with dissociation constants of order 1.0 μM .¹⁵ Crystal structures show differences in the conformation and shape of the protein in its Ca^{2+} -bound and unbound states, and previous work has demonstrated CaM gels that change shape,¹⁶ making it an ideal protein to test both the real-time and wavelength resolution of our LSPR spectrometer in response to small, reversible refractive index changes.

To immobilize calmodulin, we created a protein construct consisting of a CaM domain sandwiched between two cutinase domains, with the N-terminal cutinase rendered inactive through a mutation. The active C-terminal cutinase reacts with a phosphate ligand on the monolayer to give a covalent, site-specific attachment to the nanoparticle.¹⁷ The design of this construct confers two benefits: (1) CaM is uniformly oriented at the surface, with the cutinase acting as a spacer molecule to reduce substrate interference and more closely approximate a solution-phase protein, and (2) the N-terminal cutinase domain provides an additional mass of 22 kDa, creating a more significant change in the overall protein packing density when treated with calcium. The λ_{max} of the LSPR sensor was monitored in real-time as CutCaMCut bound to the SAM, demonstrating a shift of 3.63 nm in aqueous buffer and a noise level of 4×10^{-3} nm (Figure 1B). Spectra measured in a N_2 environment before and after this immobilization step show an increase in the extinction intensity and a $\Delta\lambda_{\text{max}}$ of +26 nm,

[†] Northwestern University.

[‡] University of Chicago.

[§] Argonne National Laboratory.

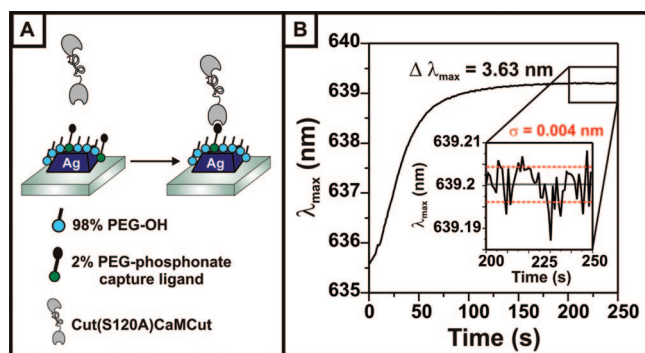


Figure 1. (A) Schematic representation of the binding of the CutCaMCut fusion protein to a phosphonate functionalized Ag nanoparticle sensor; (B) plot of changes in λ_{\max} in real-time as CutCaMCut binds to the sensor surface in solution. Inset: Closeup after the reaction is complete, showing a noise level of 4×10^{-3} nm averaged over 50 s.

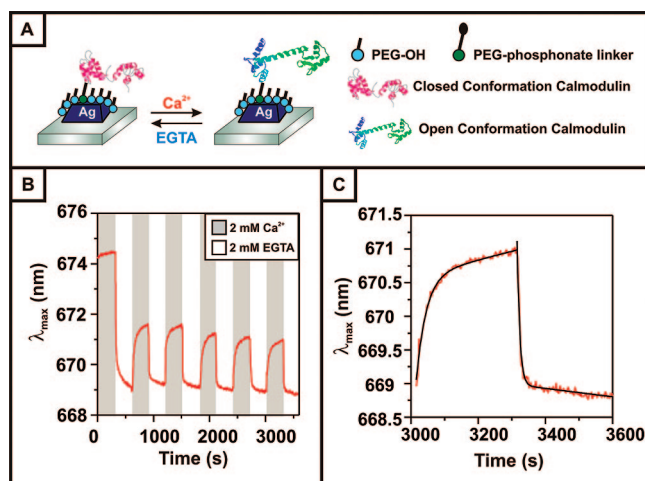


Figure 2. (A) Schematic representation of the reversible conformational changes of CutCaMCut immobilized on the LSPR nanosensor. (B) Plot of changes in the extinction maximum (1 Hz collection) of the sensor as the buffer is cycled between 2 mM CaCl_2 and 2 mM EGTA, a calcium chelator. (C) Closeup of one $\text{CaCl}_2/\text{EGTA}$ cycle, with an exponential fit of $\lambda_{\max} = \lambda_{\max(0)} + A \exp(-t/\tau) + B*t$ (black) to the experimental data (red), where $\tau_{(\text{open})} = 30$ s, $\tau_{(\text{close})} = 8$ s, and $|B| < 0.0013$ nm/s.

verifying that CutCaMCut is bound to the surface (Supporting Information).

We next tested whether the HR LSPR spectrometer could detect the conformational changes of calmodulin that accompany Ca^{2+} binding. The λ_{\max} was monitored while exposing the sensor to alternating cycles of 2 mM CaCl_2 followed by 2 mM EGTA in 20 mM Tris buffer at pH 7.4 (Figure 2A). We expected that as calmodulin opened or closed in response to Ca^{2+} , the λ_{\max} of the LSPR sensor would reversibly shift as the center-of-mass of the calmodulin localizes further into and out of the LSPR sensing region. Indeed, the λ_{\max} shifted to the red in the presence of Ca^{2+} (open conformation) and to the blue in response to Ca^{2+} chelation by EGTA (closed conformation). With each alternating buffer cycle, the λ_{\max} shifted an average of 2.197 ± 0.176 nm after the initial incubation (Figure 2B). Exponential fits to the data with a correction for linear baseline drift reveal an opening rate of ~ 0.034 s^{-1} and a closing rate of ~ 0.127 s^{-1} (Figure 2C). Furthermore, two controls were performed to verify that the LSPR shifts observed were the result of conformational changes. In the first, Ag nanoparticles with a phosphonate-terminated SAM and no calmodulin on the surface were subjected to CaCl_2 and EGTA cycles. In the second, Ag nanoparticles functionalized with the noncalcium sensi-

tive cutinase–cutinase construct were also exposed to consecutive CaCl_2 and EGTA cycles. Both controls showed a small continuous baseline drift due to solvent annealing, but minimal Ca^{2+} -modulated changes in λ_{\max} , verifying that the observed extinction shifts result from calmodulin conformational changes and not refractive index changes in the bulk media (Supporting Information).

In addition to demonstrating reproducible Ca^{2+} -dependent plasmonic modulations, the HR LSPR nanosensor provides information about the orientation and dynamics of the CutCaMCut system. Using the LSPR response model,⁹ the red shift upon Ca^{2+} exposure indicates that CutCaMCut reorients in a way that results in a higher overall packing density close to the nanoparticle surface. In addition, analysis of the real-time modulations reveals a closing rate ~ 4 times faster than the opening rate. Published rates of conformational changes for solution-phase calmodulin reflect both a faster and a more closely matched time scale between opening and closing rates. This discrepancy may be the result of the surface-bound nature of the protein and/or the presence of the fused cutinase domains. More detailed investigations are underway to determine the effect of calcium ion concentration on the rate of conformational changes.

These results mark the first time that a LSPR sensor has exhibited reversible spectral modulations in response to the changing conformation of an unlabeled protein. We have demonstrated that the calcium-induced change in λ_{\max} of approximately 2.2 nm is far greater than the noise level ($S/N \sim 5 \times 10^2$), label-free, and can be measured over long periods of time because the particles do not bleach. In addition, the combination of reversibility, high S/N ratio, and long-term stability of this real-time HR LSPR sensor make it a valuable tool for studies of protein orientation and structure, with potential future applications in drug discovery and disease research.

Acknowledgment. This research was supported by the National Science Foundation (Grants EEC-0647560, CHE-0414554, DMR-0520513, and BES-0507036), the National Cancer Institute (1 U54 CA119341-01), a Ruth L. Kirschstein National Research Service Award (5 F32 GM077020) to J.N.A., a George W. Beadle Postdoctoral Fellowship to Y.L., and a Ryan Fellowship to W.P.H.

Supporting Information Available: Experimental details and data not shown in the paper. This material is available free of charge via the Internet at <http://pubs.acs.org>.

References

- (1) Ishima, R.; Torchia, D. A. *Nat. Struct. Biol.* **2000**, *7*, 740–743.
- (2) Heyduk, T. *Curr. Opin. Biotechnol.* **2002**, *13*, 292–296.
- (3) Atwater, H. A. *Sci. Am.* **2007**, *296*, 56–63.
- (4) Ozbay, E. *Science* **2006**, *311*, 189–193.
- (5) Willets, K. A.; Van Duyne, R. P. *Annu. Rev. Phys. Chem.* **2007**, *58*, 267–297.
- (6) Sonnichsen, C.; Reinhard, B.; Liphardt, J.; Alivasatos, A. P. *Nat. Biotechnol.* **2005**, *23*, 741–745.
- (7) Yonzon, C. R.; Jeoung, E.; Zou, S.; Schatz, G. C.; Mrksich, M.; Van Duyne, R. P. *J. Am. Chem. Soc.* **2004**, *126*, 12669–12676.
- (8) Riboh, J.; Haes, A.; McFarland, A. D.; Ranjit, C.; Van Duyne, R. P. *J. Phys. Chem. B* **2003**, *107*, 1772–1780.
- (9) Haes, A. J.; Chang, L.; Klein, W. L.; Van Duyne, R. P. *J. Am. Chem. Soc.* **2005**, *127*, 2264–2271.
- (10) Chah, S.; Kumar, C.; Hammond, M.; Zare, R. N. *Anal. Chem.* **2004**, *76*, 2112–2117.
- (11) Kang, T.; Hong, S.; Choi, I.; Jun Sung, J.; Kim, Y.; Hahn, J.; Yi, J. *J. Am. Chem. Soc.* **2006**, *128*, 12870–12878.
- (12) Haes, A. J.; Zhou, S.; Schatz, G. C.; Van Duyne, R. P. *J. Phys. Chem. B* **2004**, *108*, 109–116.
- (13) Dahlin, A. B.; Tegenfeldt, J. O.; Hook, F. *Anal. Chem.* **2006**, *78*, 4416–4423.
- (14) McFarland, A. D.; Van Duyne, R. P. *Nano Lett.* **2003**, *3*, 1057–1062.
- (15) Linse, S.; Helmersson, A.; Forsen, S. *J. Bio. Chem.* **1991**, *266*, 8050–8054.
- (16) Murphy, W. L.; Dillmore, W. S.; Modica, J.; Mrksich, M. *Angew. Chem.* **2007**, *46*, 3066–3069.
- (17) Hodneland, C. D.; Lee, Y.; Min, D.; Mrksich, M. *Proc. Natl. Acad. Sci. U.S.A.* **2002**, *99*, 5048.

JA7109037